South African Journal of Geomatics, Vol. 14. No. 1, February 2025

An analysis of the relationship of land surface temperature with modified normalized difference water index and normalized difference built-up index in Hyderabad City, India

Subhanil Guha*, Himanshu Govil
Department of Applied Geology, National Institute of Technology, Raipur, Chhattisgarh, India
*Corresponding author: **subhanilguha@gmail.com**

DOI: https://dx.doi.org/10.4314/sajg.v14i1.9

Abstract

The study analyses the respective relationships between two independent variables, namely, modified normalized difference water index (MNDWI) and normalized difference built-up index (NDBI), and the dependent variable, land surface temperature (LST) in Hyderabad City, southern India. The study used Landsat data applicable to the dry winter season and Pearson's linear correlation coefficient for the correlation analyses. Results show that the LST values for the respective images are also positively correlated. The study also finds that LST shows a moderate negative relationship with MNDWI (average r = -0.57) and a moderate positive relationship with NDBI (average r =0.55). Because the dry winter season affects urban land surface materials in a particular way, built-up areas tend to enhance LSTs in winter, while in this same season, water surfaces tend to reduce LSTs. The study could contribute significantly to sustainable urban landscape planning.

***Keywords**: Land surface temperature; Modified normalized difference water index; Normalized difference built-up index.*

1. Introduction

Nowadays, land surface temperature (LST) estimation is considered the most important procedure to consider in the study of thermal infrared remote sensing, where the thermal status of varying land use/land cover (LULC) types may control the generation of the heat island effect in mixed urban landscapes (Mirzaei, 2015; Zhao *et al*., 2016; Pandey *et al*., 2023a, 2023b, 2023c). Various spectral indices based on different bands of satellite images have been applied in LST-related research to evaluate the changing orientation of LST in various types of physical and cultural landscapes (Peng *et al*., 2016; Guha *et al*., 2022, 2023; Pandey *et al*., 2022a, 2022b). Several recent articles that are relevant to this study have described correlation analyses between spectral indices and LST in different cities (Lopez *et al*., 2017; Pearsall 2017; Guha and Govil, 2022a, 2022b, 2023).

Currently, the relationships between various normalized difference spectral indices and LST and are being constructed using thermal infrared remote sensing. Examples include the MNDWI-LST relationship (Guha and Govil, 2022a; Mondal *et al*., 2021; Taripanah and Ranjbar, 2021) and the NDBI-LST relationship (Feng *et al*., 2018; Filho *et al*., 2019; Son *et al*., 2020).

The spectral indices in the above-mentioned studies were generated by using different spectral bands of remotely-sensed data. LST respond differently to different types of LULC. LST depends heavily on various types of LULC: built-up areas, dry soils, rocks, metalled roads, and concrete infrastructures enhance LST values, whereas waterbodies, wetlands, forests, grasslands, scrubland and cultivated land tend to reduce LST values. The condition and extent of these different types of land use/land cover vary according to the seasons. Consequently, the strength of these MNDWI-LST and NDBI-LST relationships can vary seasonally.

The current study analyses the nature and strength of the respective relationships between MNDWI and LST and between NDBI and LST in the winter season of 2020-21. The primary objective of the research is to analyse the status of the respective relationships between MNDWI-LST and NDBI-LST in the winter season of 2020-21.

The study area that was selected to analyse the respective relationships between MNDWI and LST and between NDBI and LST, and, in fact for the entire research project, was Hyderabad City − the multifunctional capital city of Telengana province and the sixth-largest city in India. The above-mentioned factors, namely an urban built-up environment, together with the fact that the city is not influenced by harsh environmental conditions and that it is covered by a large percentage of water bodies and vegetation within its boundaries − all of which contribute to the nature and extent of the land use/land cover types relevant to this study that made it an ideal choice for this research.

2. Study area and data

Hyderabad City is located along the banks of the Musi River. It is located between latitudes, 17º12'01" N and 17º36'06" N, and between longitudes, 78º10'02" E and 78º39'02" E (Figure 1). It has an average elevation of 540 m. Within its domain, the city has several artificial lakes. Overall, the city is under a tropical savannah (Aw) type of climate. The average annual temperature range is 27ºC and the average annual precipitation is 170 cm. Over recent years, the rate of urbanisation

has been high. Hyderabad is the fourth most populous city and the sixth most populous urban agglomeration in India.

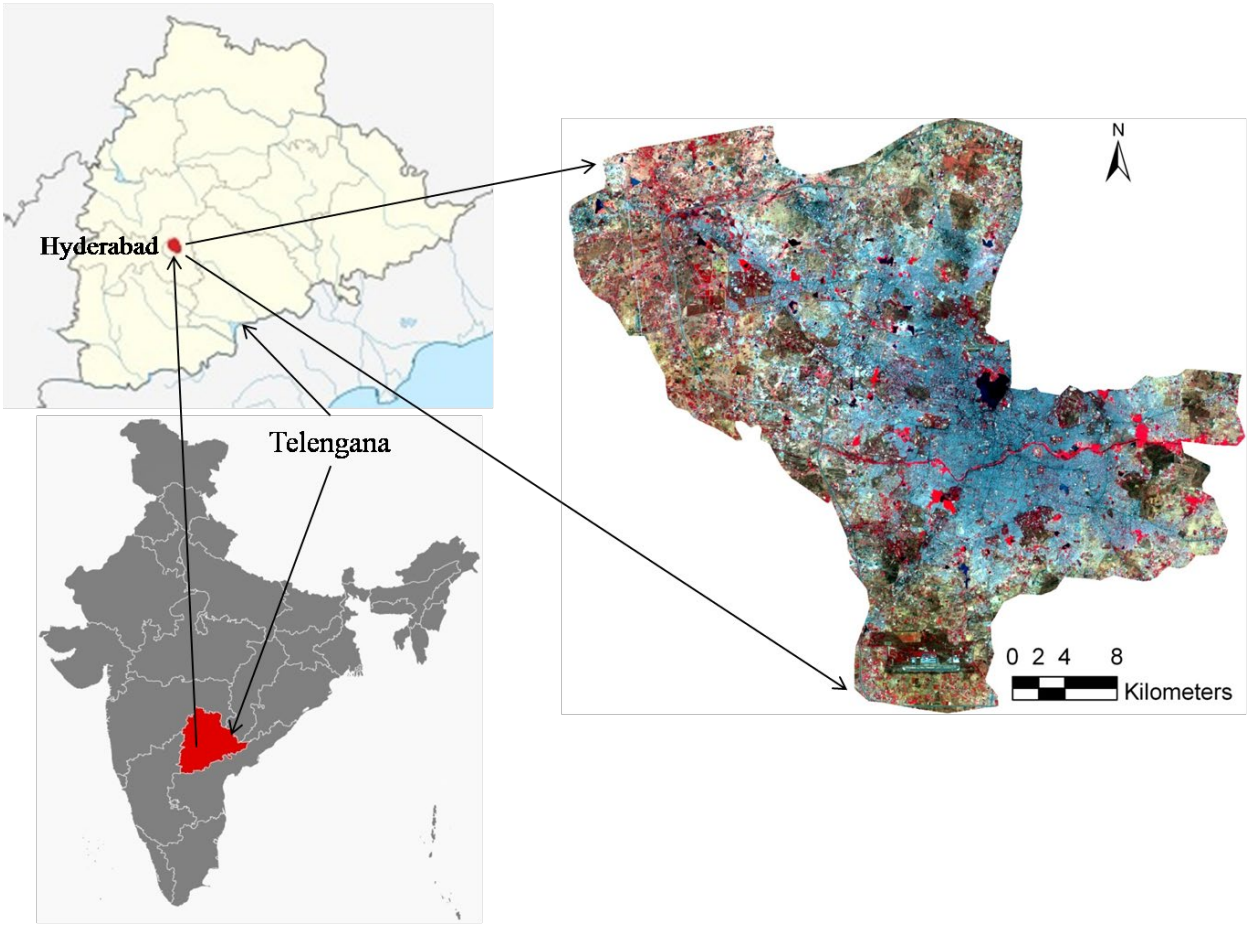

Figure 1. Location of the study area.

Table 1. Specification of the used Landsat satellite images of the winter season, 2020-21.

Landsat scene ID	Date of acquisition	Coordinated universal time (UTC)	Path/Row	Sun elevation (°)	Sun azimuth (°)	Cloud cover (%)	Earth-Sun distance (astronomical unit)	Resolution of VNIR bands (m)	Resolution of TIR bands (m)
LC81440482020347LGN00	2020-12-12	05:10:01	144/048	43.86	150.51	0.20	0.98	30	120
LC81440482020363LGN00	2020-12-28	05:09:58	144/048	42.78	148.50	1.79	0.98	30	120
LC81440482021013LGN00	2021-01-13	05:09:52	144/048	43.36	145.24	4.76	0.98	30	120
LC81440482021029LGN00	2021-01-29	05:09:48	144/048	45.55	141.03	5.82	0.98	30	120

Four 2020-21 winter season Landsat 8 satellite imageries of Hyderabad City were taken from the United States Geological Survey (http://earthexplorer.usgs.gov/) for the purposes of this study (Table 1). All the images were taken at virtually the same time. Moreover, the Google Earth Image (https://earth.google.com/web/) verified the classified images of the various LULC types considered in this study. The entire research project was processed in ERDAS Imagine and ArcGIS software.

3. Methodology

The study aimed to analyse the respective relationships between MNDWI and LST and between NDBI and LST in the study area in terms of four 2020-21 winter images. The satellite data acquired from Landsat-8 Operational Land Imager (OLI) and Thermal Infrared Sensor (TIRS) were organized into a subset to limit the data size. Because the TIR band of the Landsat 8 TIRS image (band 10) has a spatial resolution of 100 m, it was resampled using the nearest neighbour algorithm with a pixel size of 30 m to match the optical bands of the Landsat 8 OLI image.

3.1. Description of MNDWI and NDBI

The major LULC (land use/ land cover) types in the urban landscape are green vegetation, water, wetland, barren land, and settlements (built-up areas). Thus, MNDWI (Xu 2006) and NDBI (Zha *et al.,* 2003) were the chosen spectral indices for this study as these retrieve waterbody and built-up area data (Table 2). The Green and Shortwave Infrared 1 (SWIR1) bands were used to compute MNDWI, while the SWIR1 and NIR bands were used to determine NDBI. On the other hand, the TIR band was used with the Red and NIR bands to estimate land surface emissivity and LST. After determining the LULC indices and the LSTs for all four winter images, the MNDWI-LST and NDBI-LST relationships were determined for each image.

Table 2. A detailed description of the MNDW and NDB Indices.

Acronym	Description	Formulation	References
MNDWI	Modified normalized difference water index	Green-SWIR1/Green+SWIR1	Xu 2006
NDBI	Normalized difference built-up index	SWIR1-NIR/SWIR1+NIR	Zha et al. 2003

3.2. LST estimation

LST computation by using the Landsat TIR band follows several sequential algorithms. Firstly, spectral radiance is calculated by applying Equation 1 (Artis and Carnahan, 1982):

$$L_\lambda = RadianceMultiBand \times DN + RadianceAddBand \quad (1)$$

L_λ = the spectral radiance in $Wm^{-2}sr^{-1}mm^{-1}$.

After that, the at-sensor brightness temperature is estimated by applying Equation 2:

$$T_B = \frac{K_2}{\ln((K_1 / L_\lambda) + 1)} \quad (2)$$

Where, T_B = brightness temperature in Kelvin (K), L_λ = spectral radiance in $Wm^{-2}sr^{-1}mm^{-1}$; K_2 and K_1 = calibration constants.

Thereafter, fractional vegetation is computed by applying Equation 3 (Carlson and Ripley, 1997).

$$F_v = \left(\frac{NDVI - NDVI_{min}}{NDVI_{max} - NDVI_{min}} \right)^2 \quad (3)$$

Where, $NDVI_{min}$ = minimum NDVI, $NDVI_{max}$ = maximum NDVI. F_v = fractional vegetation.

Next, land surface emissivity ε is computed by applying Equation 4 (Sobrino *et al*., 2001, 2004):

$$\varepsilon = 0.004 * F_v + 0.986 \quad (4)$$

Where, ε = surface emissivity.

Finally, LST is computed by applying Equation 5 (Weng *et al*., 2004):

$$LST = \frac{T_B}{1 + \left(\lambda \sigma T_B / (hc)\right) \ln \varepsilon} \quad (5)$$

Where, λ = effective wavelength, σ = Boltzmann constant ($1.38x10^{-23}$ J/K), h = Plank's constant ($6.626x10^{-34}$ Js), c = velocity of light in a vacuum ($2.998x10^{-8}$ m/sec), ε = emissivity.

The detailed picture of the methodology is shown by a flowchart in Figure 2:

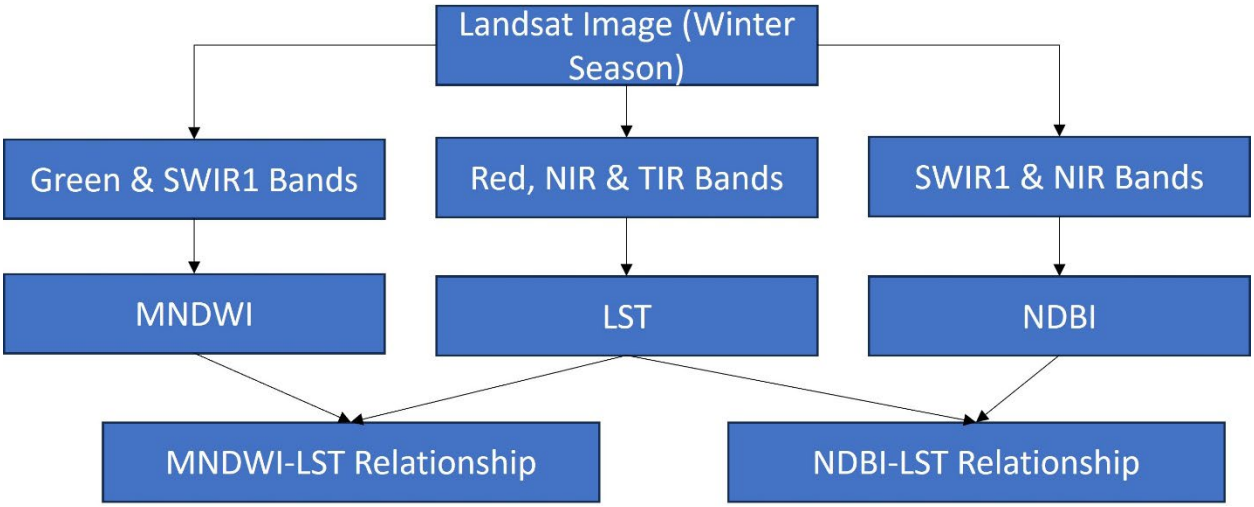

Figure 2. Flowchart showing the methodology of the present study.

4. Results

4.1. Spatial distribution (status) of LSTs

The spatial distribution (status) of LSTs observed on the four respective dates in the 2020-21 winter season as it is indicated in Figure 3. Furthermore, because the winter weather conditions do not vary significantly for the four respective dates researched, a stable condition is also noticed in the mean, minimum, and maximum LST values (Table 3). In each image, the northwestern and southeastern parts of Hyderabad experience higher LSTs. Owing to the presence of water and green areas, the central part of the city experiences, to a certain degree, a cooling effect.

Table 3 presents the spatial distribution of LSTs in Hyderabad City for the four dates in the winter season, 2020-21. The table shows that the minimum LSTs vary from 10.71ºC to 12.37ºC; the maximum LSTs vary from 28.79ºC to 34.41ºC; and the mean LSTs vary from 22.45ºC to 25.66ºC. As a whole, the statistics show very stable LST levels over these dates in this particular season. Hence, the range in the minimum, maximum, and mean LST values is narrow. As such, the four winter images in Table 3 show highly stable LST levels in the winter season of 2020-21. The north-western and south-eastern peripheries of the city experience higher LSTs than the central part of the city.

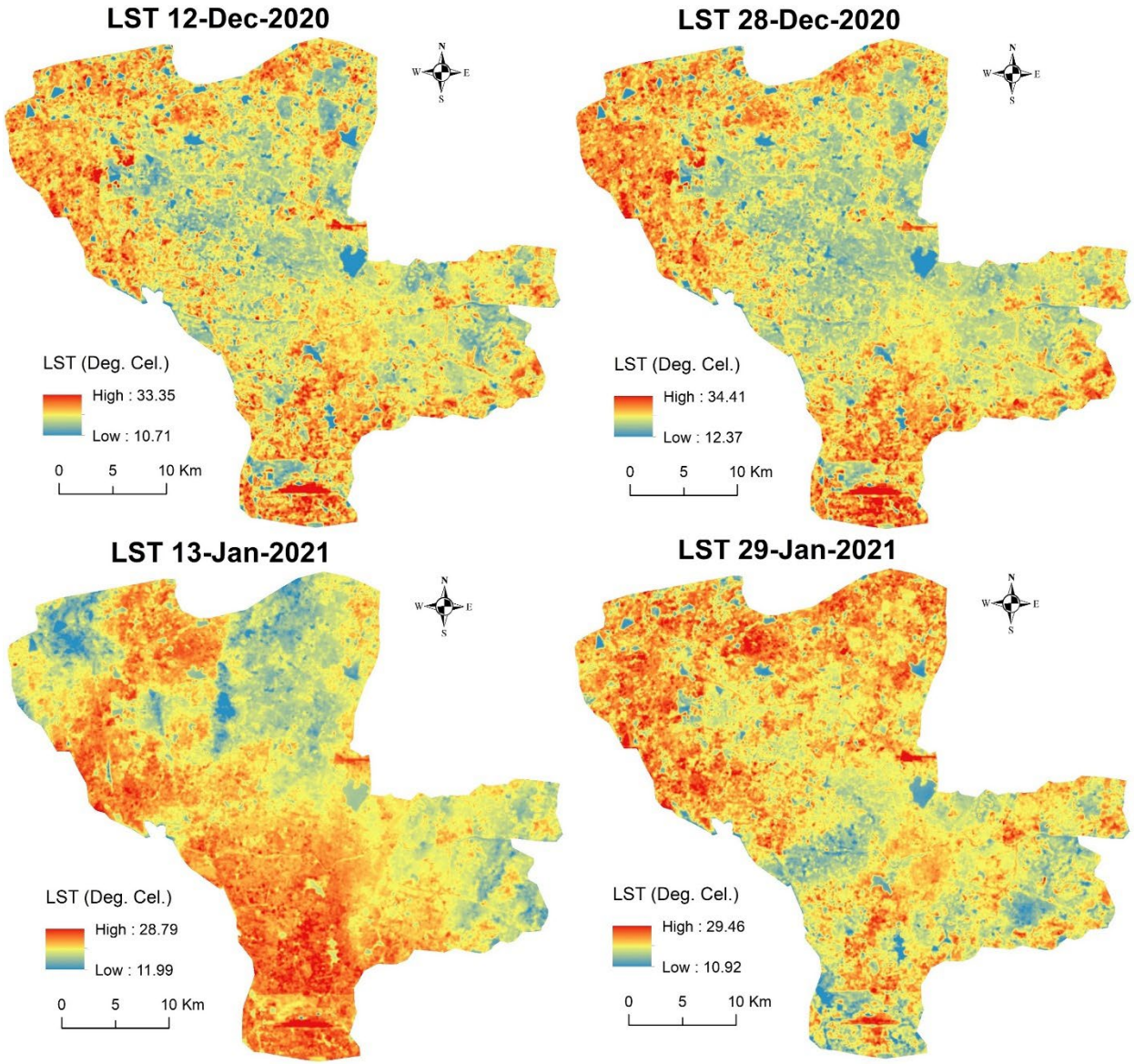

Figure 3. Spatial distribution (status)of LST (winter 2020-21).

4.2.Spatial distribution (status) of MNDWI and NDBI

Figures 4 and 5 show the spatial distribution (status) of the MNDW and NDB indices for the 2020-21 winter images. In all of the images, much smaller deviations from the norm are seen in the indices. This indicates that the weather conditions and the nature of the surface materials in the study area do not vary according to time (the dates in this context). While the area east of the central part of Hyderabad City, and several other small patches in the city present with higher

MNDWI values, the northwest and southeast portions have lower MNDWI values. The results show an inverse relationship between MNDWI and LST and a positive relationship between NDBI and LST in terms of the spatial distribution of the respective indices/variables (MNDWI, NDBI, and LST)). The peripheral areas of the city have higher NDBI values whereas the central section of the city has lower NDBI values (Figure 5).

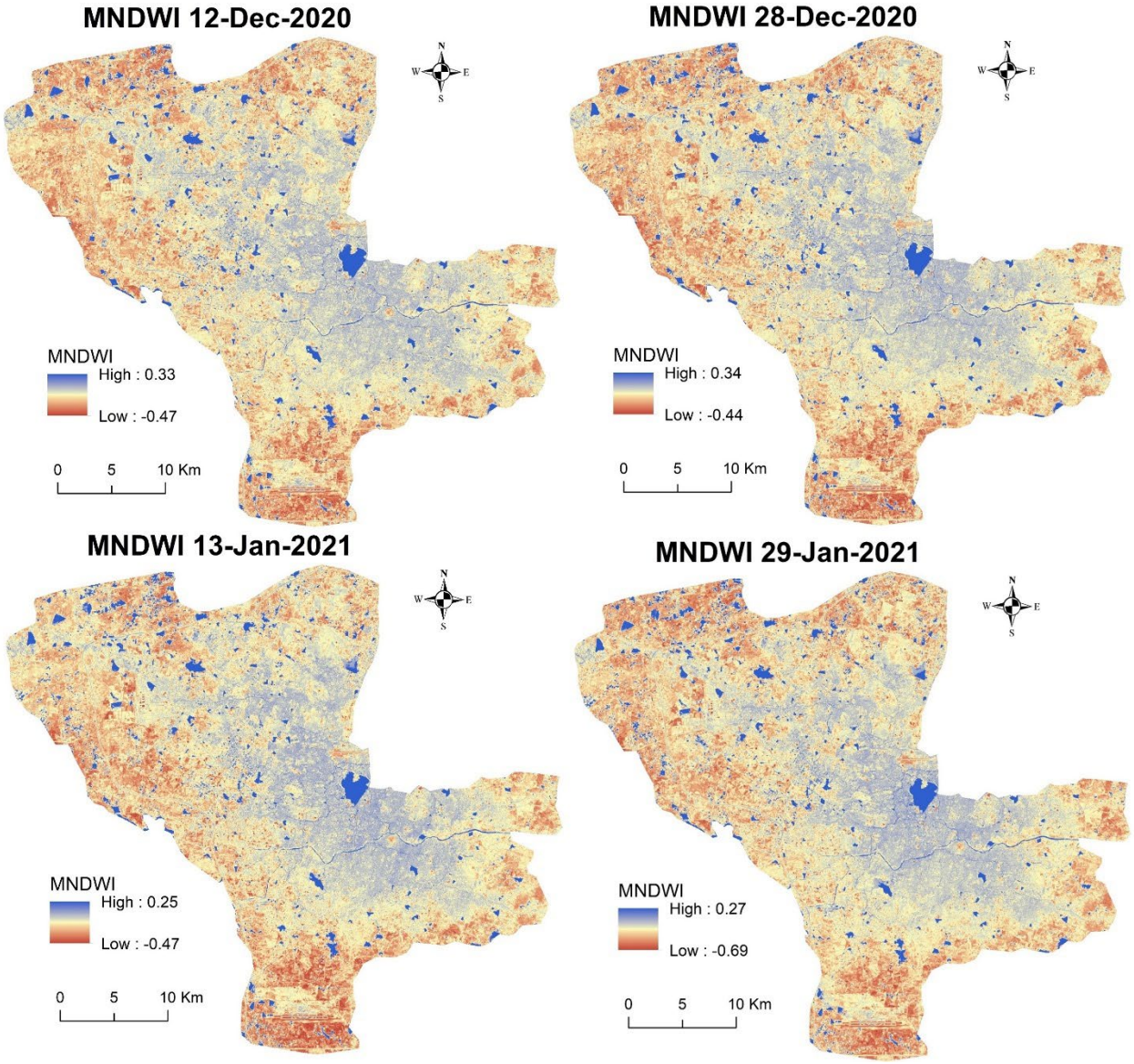

Figure 4. Spatial distribution (status) of MNDWI.

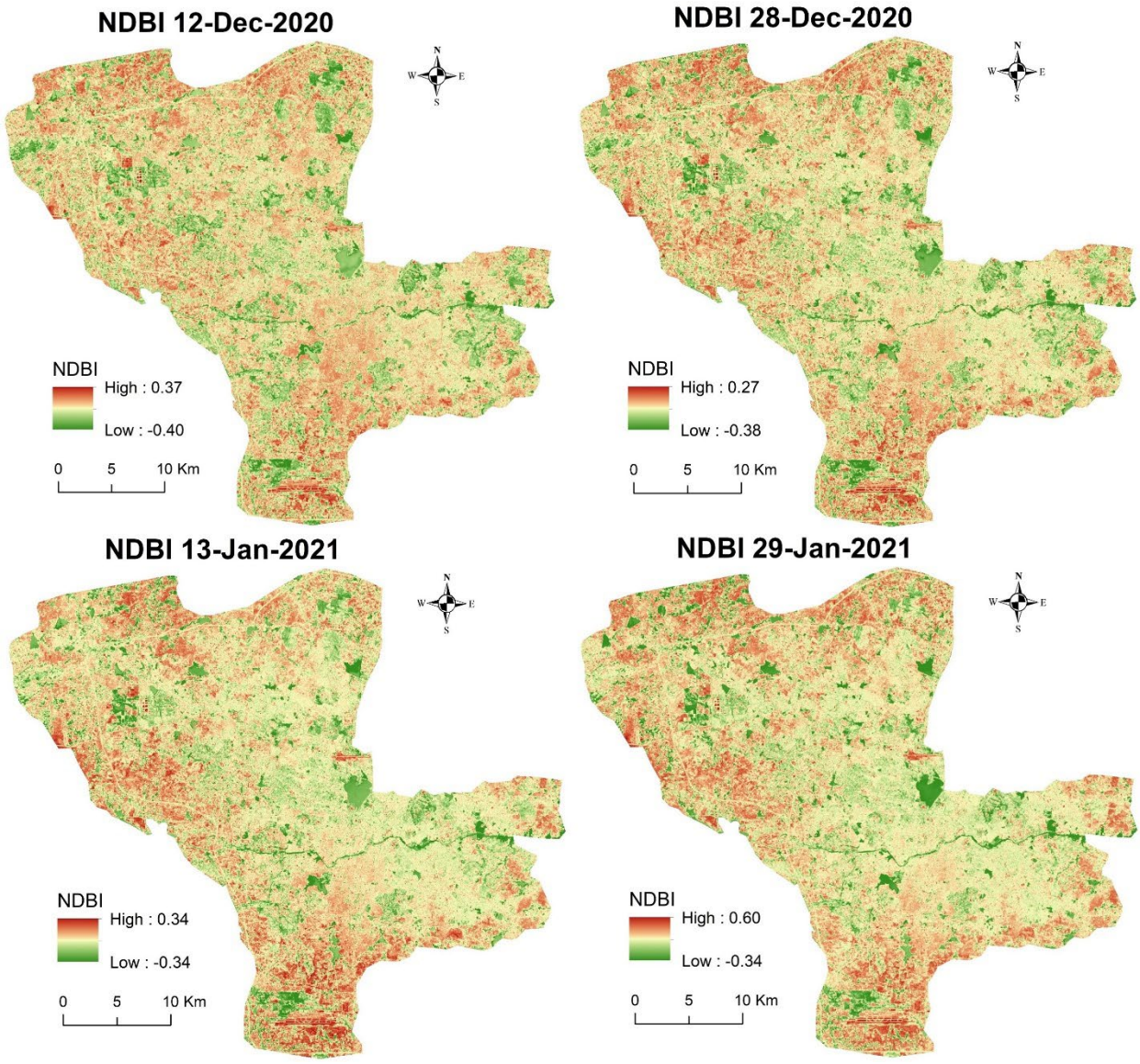

Figure 5. Spatial distribution (status) of NDBI.

Table 3 describes further details on the LST, MNDWI, and NDBI values. The range in the LST averages or means for the four dates is 3.21, which points to stable surface characteristics and weather conditions. The range in the respective means for MNDWI (-0.03) and NDBI (-0.02) is also significantly low.

Table 3. A detailed description of LST, MNDWI and NDBI.

		LST(°C)		
Date of acquisition	Min.	Max.	Mean	Std. Dev.
12-Dec-2020	10.71	33.35	25.66	1.36
28-Dec-2020	12.37	34.41	25.43	1.45
13-Jan-2021	11.99	28.79	22.45	2.46
29-Jan-2021	10.92	29.46	23.35	1.39
		MNDWI		
Date of acquisition	Min.	Max.	Mean	Std. Dev.
12-Dec-2020	-0.47	0.32	-0.11	0.07
28-Dec-2020	-0.44	0.34	-0.09	0.07
13-Jan-2021	-0.47	0.25	-0.08	0.06
29-Jan-2021	-0.69	0.27	-0.08	0.07
		NDBI		
Date of acquisition	Min.	Max.	Mean	Std. Dev.
12-Dec-2020	0.40	0.37	-0.03	0.06
28-Dec-2020	0.38	0.27	-0.02	0.06
13-Jan-2021	0.34	0.34	-0.02	0.05
29-Jan-2021	0.34	0.60	-0.01	0.05

Table 4 shows the correlation matrices in the context of the respective images and variables (correlations) in terms of dates/images. The LSTs of 12 December, 2020 and 28 December, 2020 are strongly correlated (0.94), while the strength of the correlation between 13 January, 2021 and 29 January, 2021is significantly lower (0.31). Although there is a strong correlation between the variables, a little variation is found between the associated images of these indices for December and January. For MNDWI, the images for December and January are strongly correlated and likewise, the two December images and two January images, separately. For NDBI, the images for the two January images are strong correlated as opposed to those for the two images for December.

Table 4. Correlation matrices of LST, MNDWI and NDBI.

Correlation matrix of LST				
Date of acquisition	12-Dec-2020	28-Dec-2020	13-Jan-2021	29-Jan-2021
12-Dec-2020	1.00000			
28-Dec-2020	0.93808	1.00000		
13-Jan-2021	0.52225	0.51833	1.00000	
29-Jan-2021	0.71451	0.71901	0.30581	1.00000
Correlation matrix of MNDWI				
Date of acquisition	12-Dec-2020	28-Dec-2020	13-Jan-2021	29-Jan-2021
12-Dec-2020	1.00000			
28-Dec-2020	0.93413	1.00000		
13-Jan-2021	0.89660	0.94347	1.00000	
29-Jan-2021	0.87453	0.92520	0.93551	1.00000
Correlation matrix of NDBI				
Date of acquisition	12-Dec-2020	28-Dec-2020	13-Jan-2021	29-Jan-2021
12-Dec-2020	1.00000			
28-Dec-2020	0.89978	1.00000		
13-Jan-2021	0.82908	0.92005	1.00000	
29-Jan-2021	0.74574	0.87317	0.91811	1.00000

Table 5 presents the correlation coefficients for the MNDWI-LST (negative) and NDBI-LST (positive) relationships, respectively. If the average correlation coefficient values are considered, it is seen that there is a moderate correlation (-0.57) between MNDWI and LST for the four winter images. The December images (-0.64) reflect a stronger correlation between the two variables than the January images (-0.48). For NDBI, the December images (0.60) reflect stronger correlations between the two variables than those for the January images (0.49). Overall, it can be said that the MNDWI builds stronger correlations with LST than the NDBI.

Table 5. Correlation coefficients (*r*) of MNDWI-LST and NDBI-LST correlation analyses.

Date of acquisition	MNDWI-LST	NDBI-LST
12-Dec-2020	-0.60947	0.60043
28-Dec-2020	-0.67835	0.59933
13-Jan-2021	-0.44666	0.41760
29-Jan-2021	-0.52907	0.57334
Average	-0.56588	0.54767

The results of the entire study show that LST is comfortably related to MNDWI and NDBI in the winter season. Throughout the study, the relationship between MNDWI and LST in the winter is a moderate inverse (negative) relationship (average correlation coefficient is -0.57). This signifies the validity of our research results. Ma and Peng (2022) showed that LST correlates moderately and inversely (negatively) (-0.63) with MNDWI in Kunming, China. Likewise, according to Taripanah and Ranjbar (2021), the relationship between the two variables proved to be negative in their study of Sepidan County, Iran. Guha and Govil (2021) also showed that LST and MNDWI are negatively correlated in Raipur, India. Moreover, Mashiella *et al*. (2020) established that LST has a strong inverse (negative) correlation (-0.78) with MNDWI in Sleman Regency, Indonesia.

In our current study, the NDBI-LST correlation is stable and moderately positive (average correlation coefficient is 0.55) in the winter season. This result significantly supports many other earlier NDBI-LST-related research works conducted in Fuzhou City, China (Zhang *et al*., 2009), Bahir Dar City, Ethiopia (Balew and Korme, 2020), Melbourne City, Australia (Jamei *et al*. 2019), the Chattogram metropolitan area in Bangladesh (Roy et al. 2020), San Salvador City, El Salvador (Son *et al*. 2020), Kunming, China (Chen and Zhang 2017), Wuhan City, China (Chen *et al*. 2013).

5. Conclusion

This study analysed the respective spatial relationships between MNDWI and LST and between NDBI and LST on the basis of four winter Landsat 8 satellite images of Hyderabad City. During

the entire period, the relationships between the respective variables, MNDWI, NDBI, and LST, were found to be stable and therefore, consistent. Our study found that the peripheral part of the city is heated to a greater extent than the central part of the city. This is due to the preponderance of a bare earth surface and dry soils in those parts. Furthermore, the respective relationships between MNDWI and LST and between NDBI and LST were quantified as follows: the MNDWI-LST relationship/correlation was found to be a moderate inverse (negative) relationship, whereas the NDBI-LST relationship/correlation was found to be a moderate positive relationship.

Acknowledgments

The authors are indebted to the United States Geological Survey (USGS) for the freely downloadable satellite data.

Declaration

This article did not involve any human participants.

Competing interests

The authors declare that they have no competing interests.

Funding

No funding sources were available to the authors.

Availability of data and material

The data that support the findings of this study are openly available in the Earth Explorer website of USGS at https://earthexplorer.usgs.gov/.

6. References

Ali JM, Marsh SH, Smith MJ (2017) A comparison between London and Baghdad surface urban heat islands and possible engineering mitigation solutions. *Sustainable Cities and Society,* 29: 159-168. Retrieved from: https://doi.org/10.1016/j.scs.2016.12.010

Artis DA, Carnahan WH (1982) Survey of emissivity variability in thermography of urban areas. *Remote Sensing of Environment*, *12*(4): 313–329.

Balew A, Korme T (2020) Monitoring land surface temperature in Bahir Dar city and its surroundings using Landsat images. *Egyptian Journal of Remote Sensing and Space Sciences.* Retrieved from: https://doi.org/10.1016/j.ejrs.2020.02.001

Carlson TN, Ripley DA (1997) On the Relation between NDVI, Fractional Vegetation Cover, and Leaf Area Index. *Remote Sensing of Environment*, *62*: 241-252. Retrieved from: https://doi.org/10.1016/S0034-4257(97)00104-1

Chen L, Li M, Huang F, Xu S (2013) Relationships of LST to NDBI and NDVI in Wuhan City based on Landsat ETM+ image. 2013. Sixth International Congress on Image and Signal Processing (CISP), Hangzhou, 2013, 840-845.

Chen X, Zhang Y (2017) Impacts of urban surface characteristics on spatiotemporal pattern of land surface temperature in Kunming of China. *Sustainable Cities and Society, 32*: 87-99. Retrieved from: https://doi.org/10.1016/j.scs. 2017.03.013

Feng Y, Li H, Tong X, Chen L, Liu Y (2018) Projection of land surface temperature considering the effects of future land change in the Taihu Lake Basin of China. *Global and Planetary Change*, *167*: 24-34. Retrieved from: https://doi.org/10.1016/j.gloplacha.2018.05.007

Filho WLFC, De Barros Santiago D, De Oliveira-Júnior JF, Da Silva Junior CA (2019) Impact of urban decadal advance on land use and land cover and surface temperature in the city of Maceió, Brazil. Land Use Policy, *87*: 104026. Retrieved from: https://doi.org/10.1016/j.landusepol.2019.104026

Guha S, Govil H (2023) Evaluating the stability of the relationship between land surface temperature and land use/land cover indices: a case study in Hyderabad city, India. *Geology, Ecology and Landscapes*. Retrieved from: http://dx.doi.org/10.1080/24749508.2023.182083

Guha S, Govil H (2022a) Annual assessment on the relationship between land surface temperature and six remote sensing indices using Landsat data from 1988 to 2019. *Geocarto International*, *37*(15): 4292-4311. Retrieved from: https://doi.org/10.1080/10106049.2021.1886339

Guha S, Govil H (2022b) Seasonal impact on the relationship between land surface temperature and normalized difference vegetation index in an urban landscape. *Geocarto International, 37*(8): 2252-2272. Retrieved from: https://doi/10.1080/10106049.2020.1815867

Guha S, Govil H, Mukherjee S (2023) Long-term evaluation of land surface temperature with bare surface index and surface vegetation index: a case study of a central Indian city. *Papers in Applied Geography*, *9*(4): 425-441. Retrieved from: https://doi.org/10.1080/23754931.2023.2240803

Guha S, Govil H, Taloor AK, Gill N, Dey A (2022) Land surface temperature and spectral indices: A seasonal study of Raipur City. *Geodesy and Geodynamics, 13*(1): 72-82. Retrieved from: https://doi.org/10.1016/j.geog.2021.05.002

Lopez JMR, Heider K, Scheffran J (2017) Frontiers of urbanization: Identifying and explaining urbanization hot spots in the south of Mexico City using human and remote sensing. *Applied Geography*, *79*: 1-10.

Ma X, Peng S (2022) Research on the spatiotemporal coupling relationships between land use/land cover compositions or patterns and the surface urban heat island effect. *Environmental Science and Pollution Research, 29*(26): 39723-39742. Retrieved from: https://doi.org/10.1007/s11356-022-18838-3

Mirzaei PA (2015) Recent challenges in modeling of urban heat island. *Sustainable Cities and Society, 19*: 200–206. Retrieved from: https://doi.org/10.1016/j.scs.2015.04.001

Mondal A, Guha S, Kundu S (2021) Dynamic status of land surface temperature and spectral indices in Imphal city, India from 1991 to 2021. *Geomatics, Natural Hazards and Risk, 12*(1): 3265-3286. Retrieved from: https://doi.org/10.1080/19475705.2021.2008023

Pandey A, Mondal A, Guha S, Singh D, Rashmi, Kundu S (2023a) Analysis of the variability in land surface temperature due to land use/land cover change for sustainable urban planning. *Journal of Landscape Ecology, 16*(3): 20-35. Retrieved from: https://doi.org/10.2478/jlecol-2023-0015

Pandey A, Mondal A, Guha S, Upadhyay PK, Rashmi (2022a) A seasonal investigation on land surface temperature and spectral indices in Imphal city, India. *Journal of Landscape Ecology, 15*(3): 1-18. https://doi.org/10.2478/jlecol-2022-0015

Pandey A, Mondal A, Guha S, Upadhyay PK, Rashmi, Kundu S (2023b) Analysis of Spectral Indices-based Downscaled Land Surface Temperature in a Humid Subtropical City. *International Journal of Image and Data Fusion*. *14*(4): 336-358. Retrieved from: https://doi.org/10.1080/19479832.2023.2252818

Pandey A, Mondal A, Guha S, Upadhyay PK, Singh D (2023c) A long-term analysis of the dependency of land surface temperature on land surface indices. *Papers in Applied Geography*. *9*(3): 279-294 Retrieved from: https://doi.org/10.1080/23754931.2023.2187314

Pandey A, Mondal A, Guha S, Upadhyay PK, Singh D (2022b) Land use status and its impact on land surface temperature in Imphal city, India. *Geology, Ecology, and Landscapes*. Retrieved from: http://dx.doi.org/10.1080/24749508.2022.2131962

Pearsall H (2017) Staying cool in the compact city: Vacant land and urban heating in Philadelphia, Pennsylvania. *Applied Geography, 79*: 84–92. Retrieved from: http://dx.doi.org/10.1016/j.apgeop.2016.12.010

Peng J, Xie P, Liu Y, Ma J (2016) Urban Thermal Environment Dynamics and associated Landscape Pattern Factors: a Case Study in the Beijing Metropolitan Region. *Remote Sensing of Environment*, *173*: 145–155.

Roy S, Pandit S, Eva EA, Bagmar MSH, Papia M, Banik L, Dube T, Rahman F, Razi MA (2020) Examining the nexus between land surface temperature and urban growth in Chattogram Metropolitan Area of Bangladesh using long-term Landsat series data. *Urban Climate*, *32*: 100593. Retrieved from: https://doi.org/10.1016/j.uclim.2020.100593

Sobrino JA, Raissouni N, Li Z (2001) A comparative study of land surface emissivity retrieval from NOAA data. *Remote Sensing of Environment, 75*(2): 256–266. Retrieved from: https://doi.org/10.1016/S0034-4257(00)00171-1

Sobrino JA, Jimenez-Munoz JC, Paolini L (2004) Land surface temperature retrieval from Landsat TM5. *Remote Sensing of Environment, 9*: 434–440. Retrieved from: https://doi:10.1016/j.rse.2004.02.003

Son NT, Chen CF, Chen CR (2020) Urban expansion and its impacts on local temperature in San Salvador, El Salvador. *Urban Climate*, *32*: 100617. Retrieved from: https://doi.org/10.1016/j.uclim.2020.100617

Taripanah F, Ranjbar A (2021) Quantitative analysis of spatial distribution of land surface temperature (LST) in relation to ecohydrological, terrain and socio-economic factors based on Landsat data in a mountainous area. *Advances in Space Research,* 68(9): 3622-3640. Retrieved from: https://doi.org/10.1016/j.asr.2021.07.008

Tucker CJ (1979) Red and photographic infrared linear combinations for monitoring vegetation. *Remote Sensing of Environment*, *8*(2): 127–150.

Weng QH, Lu DS, Schubring J (2004). Estimation of Land Surface Temperature–Vegetation Abundance Relationship for Urban Heat Island Studies. *Remote Sensing of Environment*, *89*: 467-483. Retrieved from: https://doi:10.1016/j.rse.2003.11.005

Xu H (2006) Modification of normalized difference water index (NDWI) to enhance open water features in remotely sensed imagery. *International Journal of Remote Sensing*, *27*(14): 3025–3033.

Zhang Y, Odeh IOA, Han C (2009) Bi-temporal characterization of land surface temperature in relation to impervious surface area, NDVI and NDBI, using a sub-pixel image analysis. *International Journal of Applied Earth Observation and Geoinformation,* 11(4): 256-264. Retrieved from: https://doi.org/10.1016/j.jag.2009.03.001

Zhao M, Cai H, Qiao Z, Xu X (2016) Influence of urban expansion on the urban heat island effect in Shanghai. *International Journal of Geographic Information Science*, *30*(12): 2421–2441. Retrieved from: https://doi.org/10.1080/13658816.2016.1178389

Zha Y, Gao J, Ni S (2003) Use of normalized difference built-up index in automatically mapping urban areas from TM imagery. *International Journal of Remote Sensing*, *24*(3): 583-594. Retrieved from: https://doi.org/10.1080/01431160304987